Linear Stability Analysis of a Boundary Layer with Plasma Actuators

Mark Riherd* and Subrata Roy†

Applied Physics Research Group, University of Florida, Gainesville, FL, 32611

The stability of plasma actuated boundary layers is analyzed using linear stability theory for flow wise (co-flow) and flow opposing (counter flow) operated plasma actuators. The combined wall jet/boundary layer velocity profile is discussed, important parameters are identified, and a simplified model of the base flow is proposed. This base flow is then analyzed using one-dimensional linear stability theory. Neutral stability curves have been calculated, and both stabilizing and destabilizing effects were found, which correlate strongly with the existence of an inviscid instability. A hypothesized absolute instability is also found to exist. The addition of a wall jet is found to have a profound impact on the stability of the boundary layer profile, which is compared to existing data for other boundary layer profiles. Considerations for flow control applications are discussed in order to suggest the effects for real flows.

Nomenclature

u_i	Flow velocity in the i$^{\text{th}}$ direction
p	Pressure
$\bar{u}_i$	Mean flow velocity in the i$^{\text{th}}$ direction
$\bar{p}$	Mean pressure
$\tilde{u}_i$	Disturbance flow velocity in the i$^{\text{th}}$ direction
$\tilde{p}$	Disturbance pressure
u_i'	Complex 1D disturbance flow velocity profile in the i$^{\text{th}}$ direction
p'	Complex 1D pressure profile
u_∞	Freestream velocity
u_p	Induced velocity
α	Complex spatial frequency in x_1
β	Complex spatial frequency in x_3
ω	Complex temporal frequency
c_p	Complex phase velocity, $c_p = \omega/\alpha$
c_g	Complex group velocity, $c_g = \partial\omega/\partial\alpha$
$\delta_{99\%}$	Boundary layer height where $u = 0.99u_\infty$
δ^*	Displacement boundary layer height
θ	Momentum boundary layer height
Re	Reynolds number
γ	Velocity ratio
η	Boundary layer height ratio
F	Dimensionless frequency, $F = \omega_R/Re$
i	$\sqrt{-1}$

Subscript

i	direction
I	Imaginary
R	Real

*Graduate Research Assistant, Student Member AIAA.

†Associate Professor, Associate Fellow AIAA

S	Inflection point value
$Blasius$	Corresponds to the Blasius boundary layer component of the velocity profile

I. Introduction

The process of a flow's transition to turbulence has long been a topic of study in fluid mechanics. Specifically, the flow over a flat plate with zero pressure gradient (ZPG) is particularly important, as it shares many characteristics of other more complex flows. The instability present in this flow, characterized as the Tollmien-Schlichting (TS) wave, was first theoretically explored by Tollmien[1] and Schlichting,[2] and later experimentally verified by Schubauer and Skramstead.[3]

These early studies were dependent on the assumptions of a one dimensional, parallel flow. Under these assumptions, disturbances are governed by linear equations and grow at exponential rates. One dimensional, parallel, linear stability theory was later augmented by the effects of non-parallelism.[4] A more comprehensive method taking advantage of a parabolic form of the Navier-Stokes equations was also developed (parabolized stability equations, PSE[5]), allowing for a more complete study of the boundary layer stability incorporating non-parallel and non-linear effects simultaneously. However, these methods, while not requiring as strong of assumptions about the flow, have not shown a significant difference in results for simple, nearly parallel flows such as that of the ZPG boundary layer. As such, one dimensional, parallel flow assumptions should be sufficient for the simple, nearly parallel flows examined in this study.

Using these assumptions along with linear stability theory (LST), this study examines the effect of flow-wise (co-flow) and flow opposing (counter flow) operated dielectric barrier discharge (DBD) actuators on the stability of the ZPG boundary layer flow. These devices are able to produce charged particles and a sufficiently strong electric field, which introduces a localized electrical body force that can be used to add or remove momentum from the nearby fluid.[6–8] Furthermore, these devices can be operated in a steady or duty-cycled manner, allowing them to be implemented as components of active and passive flow control systems.

Grundmann and Tropea used these devices as a method of active transition delay. They applied DBD actuators as part of a closed loop control system to cancel oncoming TS waves.[9,10] They found that DBD actuators could be used to accurately inject momentum into the boundary layer, modifying the TS waves. Gibson et al used DBD devices in a passive manner in conjunction with boundary layer suction to reduce the displacement and momentum deficit boundary layer heights and stabilize the flow.[11]

Aside from experimentation, some theoretical work has also been performed describing the momentum addition using electrical devices modifies the boundary layer and its stability properties. Albrecht et al[12] used LST and direct numerical simulation on a Lorentz force induced actuation in a boundary layer flow, which showed that with a well distributed body force mimicking wall suction, the transition can be significantly delayed. However, due to the more localized nature of the DBD actuator relative to the Lorentz force actuator, the predicted global increase in stability may or may not be physically realizable. Limited LST was performed and verified numerically and experimentally by Duchmann et al[13] for a single condition where the actuator was placed within the transitional Reynolds number regime, $Re_x \approx 270,000$ ($Re_{\delta^*} \approx 800$). While two operation modes for the plasma actuator were performed, only one was examined using LST. That study also shows that there are distinct changes in the flow stability near the plasma device, but forgoes discussion of the effects.

The goal of this study is to develop a more general understanding of how the wall jet effects seen in previous studies can be used to stabilize and destabilize a boundary layer. An extended range of parameters is considered relative to previous work. This study also intends to examine effects not seen in other studies, particularly that of the counter-flow operated plasma actuator, which has received little attention from a theoretical point of view.

II. Model of a plasma actuated flow

The presence of a DBD actuator in a boundary layer flow is known to create wall jet like effects near the surface.[8] This wall jet is created by the introduction of a body force into the fluid by the plasma actuator. This body force imparts momentum into a volume of fluid. In turn, a wall jet develops with a specific amount of momentum and a maximum velocity near the surface of the actuator.

Consider a model of the modified boundary layer where a wall jet is simply superimposed onto a boundary

layer profile (Fig. 1). While this combined profile is not a solution to the Navier-Stokes equations, it should approximate the boundary layer/wall jet velocity profile seen in other numerical and experimental studies. For the present study, a Glauert wall jet is selected as the wall jet profile,[14] and the Blasius boundary layer is selected as the boundary layer profile.[15] These two components are selected as they are both analytical solutions to the Navier-Stokes equations. Under quiescent conditions, DBD actuation will even produce a Glauert wall jet sufficiently far downstream of the body force.[16] However, it should be noted, that the similarity variables for each of these components are not the same. The superposition of these two analytical solutions is not an analytical solution of the Navier-Stokes equations, only an approximation done in order to mimic the actual flow.

In order to manipulate this model, scaling parameters are necessary. The maximum velocity of the wall jet presents itself as an important parameter. The normalized momentum injected into the boundary layer can be described as a length scale such that,

$$\delta^*_{plasma} = \int_0^\infty \frac{u_{plasma}(y)}{u_{plasma,max}} dy \tag{1}$$

The boundary layer displacement height, which measures the momentum missing in the boundary layer, can be described as a comparable length scale such that

$$\delta^*_{Blasius} = \int_0^\infty 1 - \frac{u_{Blasius}(y)}{u_\infty} dy \tag{2}$$

Comparing these two parameters with the velocity and length scales of the boundary layer, two non-dimensional parameters are arrived at.

$$\gamma = \frac{u_{plasma,max}}{u_\infty} \tag{3}$$

$$\eta = \frac{\delta^*_{plasma}}{\delta^*_{Blasius}} \tag{4}$$

where positive values of γ indicate a co-flow operated actuator and negative values of γ indicate a counter-flow operated actuator. Using these two parameters, the velocity and vertical extent of the wall jet can easily be scaled, as can be seen in Fig. 1.

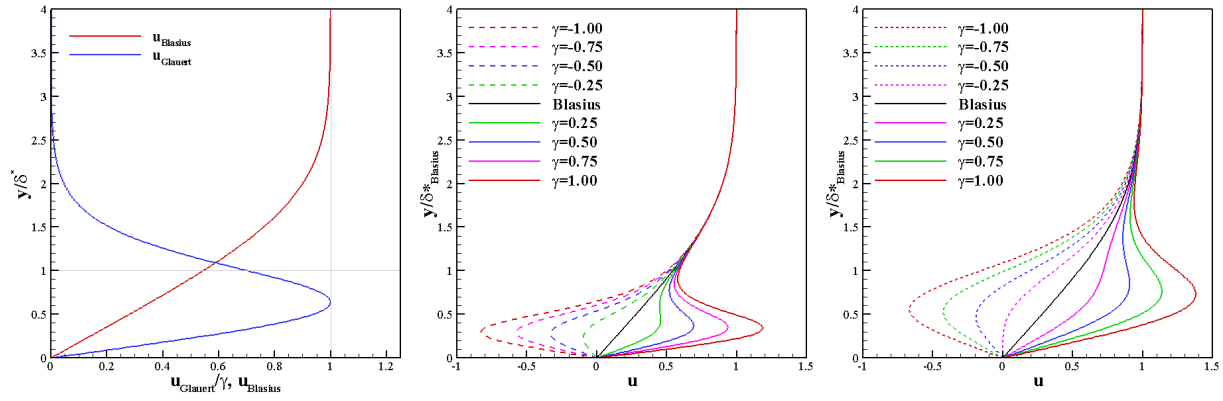

Figure 1. (a) Components of the baseline flow model and examples of the model for (b) $\eta = 0.5$ and (c) $\eta = 1.0$.

III. Linear Stability Analysis

A. Numerical model of the eigenvalue problem

Linear stability theory can be used to predict the existence and growth rates of instabilities that may manifest in the boundary layer. Though temporal instabilities are examined here, using the Gaster transformation spatial instabilities could be similarly approximated.[17]

$$u_i = \bar{u}_i + \tilde{u}_i, p = \bar{p} + \tilde{p} \tag{5}$$

$$\frac{\partial \tilde{u}_i}{\partial x_i} = 0 \tag{6}$$

$$\frac{\partial \tilde{u}_i}{\partial t} + \bar{u}_j \frac{\tilde{u}_i}{\partial x_j} + \tilde{u}_j \frac{\bar{u}_i}{\partial x_j} + \frac{\partial \tilde{p}}{\partial x_i} - \frac{1}{Re_{\delta_0^*}} \frac{\partial^2 \tilde{u}_i}{\partial x_j^2} \approx 0 \tag{7}$$

It should be noted that the non-dimensionalization here is based on δ_0^*, which is the boundary layer height of the non-actuated case at a given location in x_1.

The problem can be further simplified if several assumptions are made. First, assume that all of the disturbance quantities are wavelike in nature and can be split into the product of a disturbance profile in x_2 and a wave travelling in x_1 and x_3 such that

$$\tilde{\phi} = \phi'(x_2) \exp\left(i\left(\alpha x_1 + \beta x_3 - \omega t\right)\right) \tag{8}$$

where α, β, and ω are the angular wave numbers in x_1, x_3, and time. From this point onward, let $i = \sqrt{-1}$. Also assume that a slow developing flow can be approximated as a 1D mean flow ($u_2 = u_3 = \frac{\partial \overline{(\cdot)}}{\partial x_1} = \frac{\partial \overline{(\cdot)}}{\partial x_3} = 0$). Doing this, the problem can be formulated as the following generalized eigenvalue problem:

$$i\alpha u_1' + \frac{\partial u_2'}{\partial x_2} + i\beta u_3' = 0 \tag{9}$$

$$i\alpha \bar{u}_1 u_1' + u_2' \frac{\partial \bar{u}_1}{\partial x_2} + i\alpha p' - \frac{1}{Re}\left(-\alpha^2 u_1' + \frac{\partial^2 u_1'}{\partial x_2^2} - \beta^2 u_1\right) = i\omega u_1' \tag{10}$$

$$i\alpha \bar{u}_1 u_2' + \frac{\partial p'}{\partial x_2} - \frac{1}{Re}\left(-\alpha^2 u_2' + \frac{\partial^2 u_2'}{\partial x_2^2} - \beta^2 u_2\right) = i\omega u_2' \tag{11}$$

$$i\alpha \bar{u}_1 u_3' + i\beta p' - \frac{1}{Re}\left(-\alpha^2 u_3' + \frac{\partial^2 u_3'}{\partial x_2^2} - \beta^2 u_3\right) = i\omega u_3' \tag{12}$$

This set of equations (Eqns. 9 - 12) was then discretized onto a uniform staggered mesh.[18] A 4^{th} order accurate, centered finite difference stencil was used for the differencing over a majority of the domain. A 2^{nd} order accurate, centered finite difference scheme was used near the boundaries. Boundary layer profiles from model flow were interpolated onto the uniform mesh with 200 points spread over a domain of $4\delta_{99\%}$ based on the Blasius component of the combined velocity profile. The eigenvalues were then calculated using the inverse Rayleigh iteration method.

The code was benchmarked against that of the Poisseuille flow as discussed by Orzag.[19] The Reynolds number of this case is $Re = 10,000$. The wavenumbers are $\alpha = 1$ and $\beta = 0$. The single unstable eigenvalue is $\omega = 0.23752649 + i0.00373967$, and is considered accurate to within 8 significant digits. The calculated value of this eigenvalue was used to determine the order of accuracy of the present code. The order of accuracy of the code has been found to be somewhere between 2 and 4 (Fig. 2). The asymptotic region is reached relatively quickly for this problem. The right most point corresponds to 26 grid points, the left most corresponds to 801 grid points.

At this point it is important to note that the one dimensional linear stability theory applied here is convenient and relatively inexpensive from a computational standpoint. However, plasma actuation is known to be a localized effect. Due to the local effects, the assumptions of a slowly developing, nearly parallel flow become questionable. These assumptions should still be valid, as long as the wavelength of the disturbance (i.e. $2\pi/\alpha$) is shorter than the length scales of the developing flow. The assumptions of a nearly parallel flow are likely to be valid for a majority of the flow profiles examined here. However, for significant levels of counter flow actuation, the parallel flow assumption is likely to be violated. While the authors understand that the assumptions made may be weaker than what is desired, the results should still have some relevance to the physics involved.

B. Co-flow operated plasma actuation

Previous work[11] has shown that with the use of co-flow operated plasma actuators, it was possible to stabilize a boundary layer flow using plasma actuation. The physical mechanism identified in this study showed that plasma actuation was able to inject momentum back into the flow that had been lost by surface friction. In turn, the boundary layer heights and associated Reynolds number fell, and the flow was stabilized.

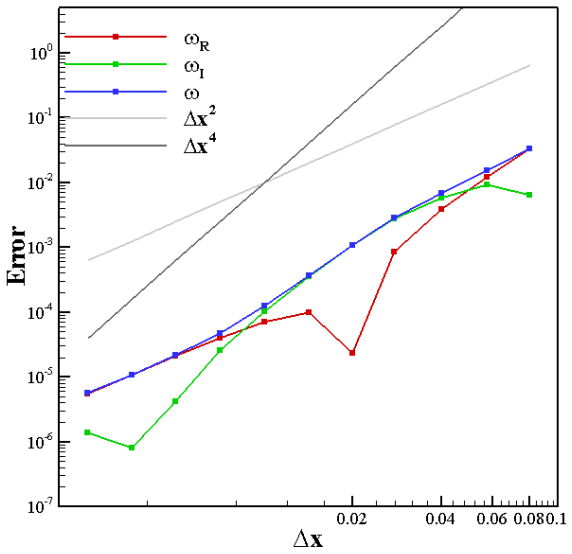

Figure 2. Grid convergence of the numerical method as compared to Orzag[19] for Poisseuille flow. $Re = 10,000,\ \alpha = 1,\ \beta = 0,\ \omega = 0.23752649 + i0.00373967$.

As part of this study, the baseline model of the flow is analyzed for wall jets of varying magnitude with a boundary layer height ratio of $\eta = 1$. Stability diagrams are shown in Fig. 3.

It can be seen that when a very small level of actuation is applied inducing only weak wall jet effects, the flow can be stabilized more than an order of magnitude higher than that of the baseline Blasius boundary layer profile. Furthermore, as the wall jet becomes stronger and stronger, flow stability is lost, and actually decreases below that of the baseline flow. These destabilizing effects can likely be attributed to an inviscid instability, which is discussed later in subsection **E**.

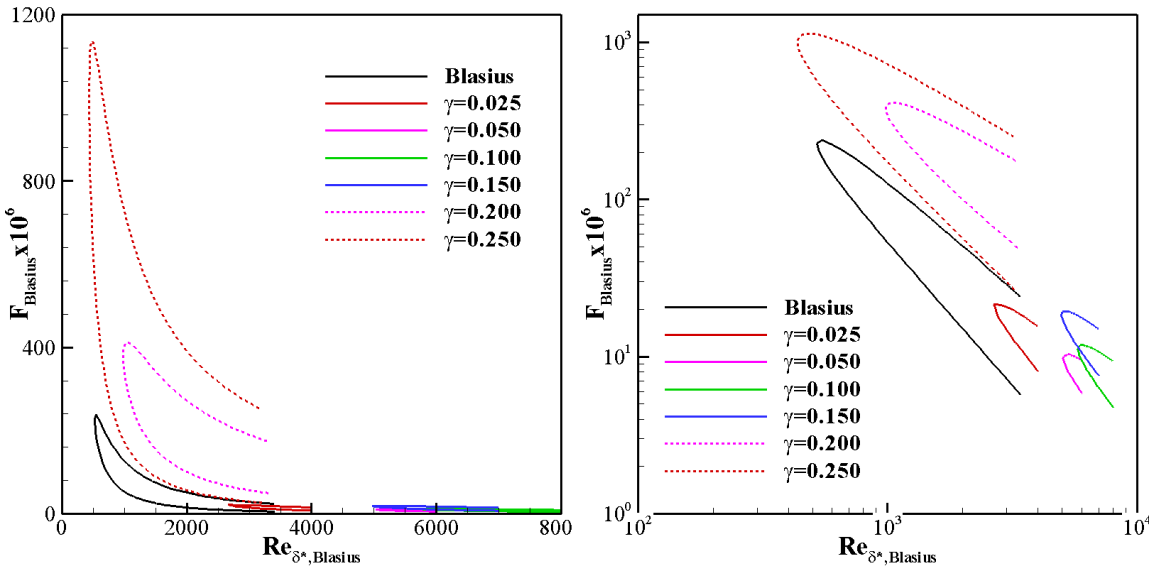

Figure 3. Nuetral stability curves for positive values of γ, where $\eta = 1.0$. Scaled by $Re_{\delta^*,Blasius}$. Data is shown for (a) linear and (b) logarithmic axis.

C. Counter-flow operated plasma actuation

To the knowledge of the authors, no work has previously been done calculating the growth rates or mapping the neutral stability curves of counter flow operated plasma actuators in a boundary layer flow. Similar parameters as the co-flow examination are performed, only with negative values of γ instead. In can be seen in the figure below that the addition of counter flow actuation is highly destabilizing, as the critical Reynolds numbers can be seen to drop 2 orders of magnitude as actuation strength is increased. Again, this instability can be linked back to a potential inviscid instability, and will be discussed in subsection **E**.

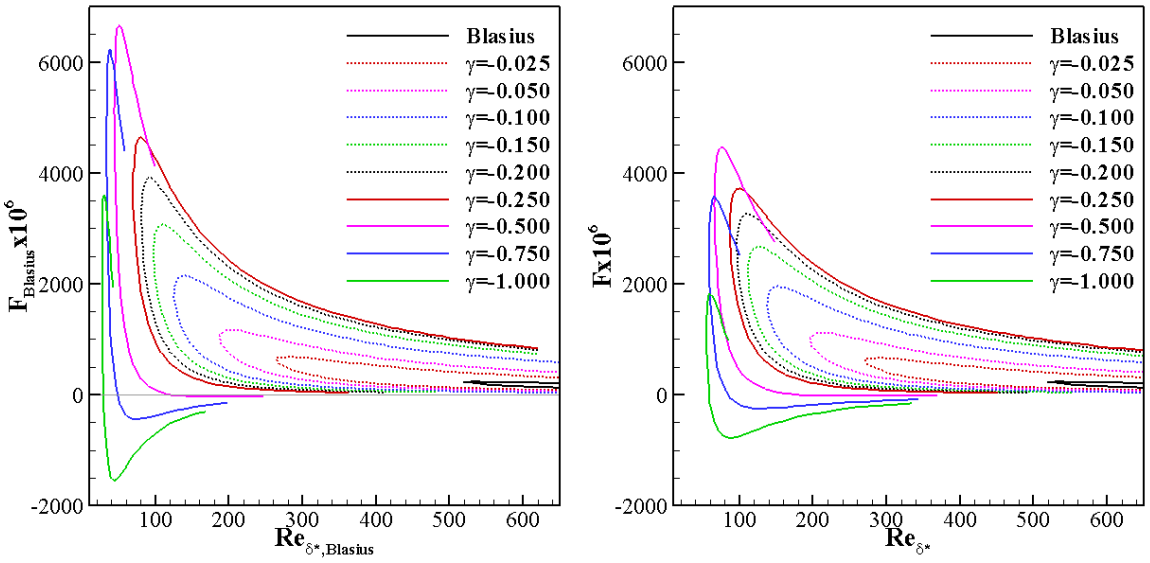

(a) (b)

Figure 4. Neutral stability curves of the counter-flow actuated flows where $\eta = 1.0$.(a) scaled by$Re_{\delta^*,Blasius}$ and (b) Re_{δ^*}.

In examining the velocity profiles of Fig. 1, it can be seen that for high enough values of the velocity ratio and low enough values of the boundary layer height ratio, flow reversal occurs. While this flow reversal is not an explicit requirement of an absolute instability, it does suggest that absolute instabilities may be present. Examining the phase speeds for the case of $\gamma = -1.0$ and $\eta = 1.0$ (Fig. 5a), there do exist eigenvalues with real phase velocities equal to zero. Examining ω_I for the same points where $c_{p,R} = (\omega/\alpha)_R = 0$, it can be seen that as the Reynolds number is increased, ω_I moves from the stable ($\omega_I < 0$) to unstable ($\omega_I > 0$) domains. Once $\omega_I > 0$, indicating that there are temporal modes which grow in place, providing further evidence for an absolute instability.

The requirements for an absolute instability as defined by Briggs[20] and Bers[21] are that:

1. There exists a dispersion relationship connecting ω and α, $\mathcal{D}(\omega, \alpha) = 0$. In the complex domains of ω and α, there must be saddle points where $\partial\omega/\partial\alpha = 0$, i.e. the group velocity equals zero.

2. The saddle points must be pinch points of an upstream and downstream travelling mode.

3. The saddle point must also be unstable. That is, $\omega_I > 0$ at the saddle point.

Constructing a 'net map' allows for the visualization of the dispersion relationship (which is a function of the velocity profile and Reynolds number) in terms of the complex values of α and ω (Fig. 6). A saddle point is immediately visible. It can be seen that as the Reynolds number is increased, the value of ω_I at this point increases from negative to positive, which satisfies the third requirement for an absolutely instability. It can be seen that above a certain critical Reynolds number, $Re_{\delta^*,abs.crit}$, the previously convective instability becomes an absolute instability.

While net maps are helpful in determining the existence of absolute instabilities, they are computationally expensive to construct. Even so, net maps were constructed for the case of $\gamma = -0.75$ in addition to $\gamma = -1.00$. From these net maps, the onset of the absolute instability was measured. Less computationally

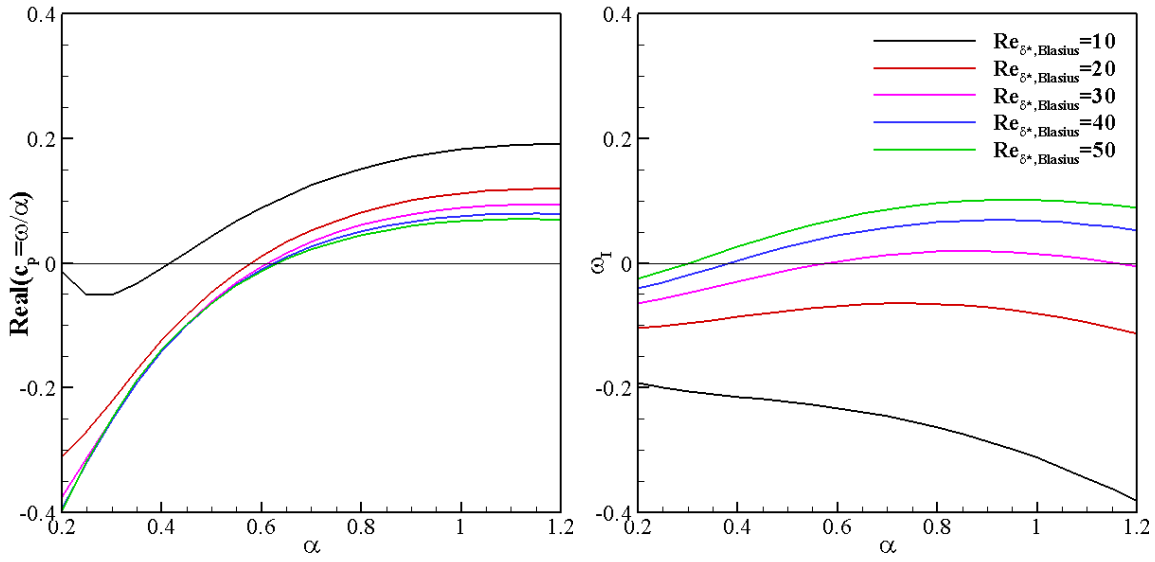

(a) (b)

Figure 5. (a) Real components of the phase velocity for selected Reynolds numbers for $\gamma = -1.0$ and $\eta = 1.0$. (b) Imaginary components of the eigenvalues, ω_I, at the same Reynolds numbers, γ, and η.

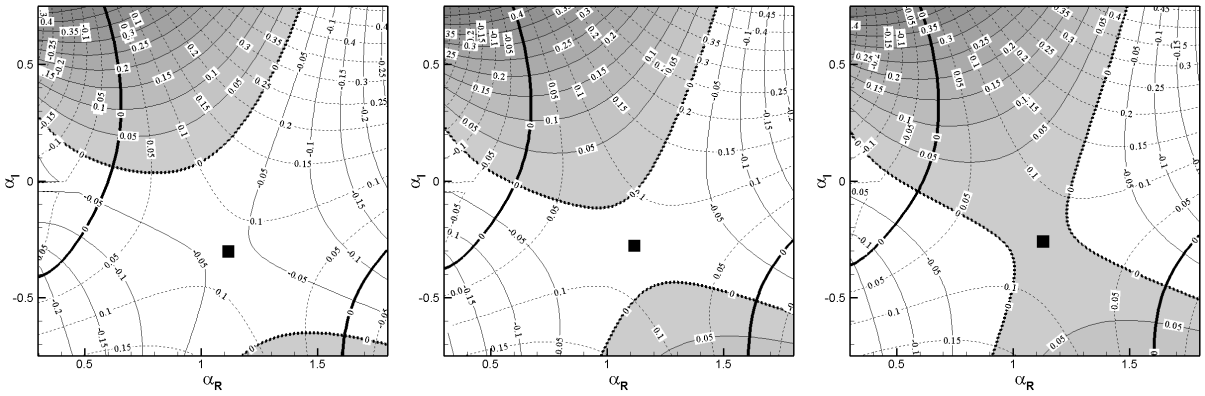

(a) (b) (c)

Figure 6. Net maps for (a) $Re_{\delta^*,Blasius} = 26$, which is absolutely stable , (b) $Re_{\delta^*,Blasius} = 30$, which is convectively unstable, and (c) $Re_{\delta^*,Blasius} = 32$, which is absolutely unstable for $\gamma = -1.0$ and $\eta = 1.0$. Solid lines indicate the contours of ω_R. Dashed lines indicate the contours of ω_I. The values of ω at the pinch points are $\omega = 0.0926214 - i0.046581$, $\omega = 0.0885969 - i0.010166$, and $\omega = 0.0867067 + i0.00496014$, which are marked by the black squares.

expensive, but approximate methods of examining the absolute instability are also examined. Values of the critical Reynolds number for zero real phase velocity and zero real group velocity from the purely temporal stability analysis are also shown in Table 1. This data shows that while the absolute instability does not exactly line up with either value, the phase velocity does give an approximate location, though the error involved is not negligible.

D. Comparison with other boundary layer profiles

It can be seen in the previous sections that co-flow and counter-flow operation of the plasma actuators has a profound effect on the boundary layer stability. However, other boundary layer profiles can be seen to have an equally strong effect on the flow stability. It is thought that there is a certain 'universal correlation' between the flow stability and the shape factor.[22] It can be seen in Fig. 7 that the critical Reynolds numbers

γ	$Re_{\delta^*,critical,Blasius}$		
	Net map	$c_{p,R}=0$	$c_{g,R}=0$
-0.750	40.7	48.2	114.0
-1.000	31.3	29.4	68.3

Table 1. Critical Reynolds numbers (based on $Re_{\delta^*,Blasius}$) of the absolute instability for two cases with reversed flow.

reached as part of this study mimic the critical stability (of the convective instability) of other boundary layer when compared via the shape factor, $H = \delta^*/\theta$. It can be seen that the destabilizing effects of the counter-flow actuation are in line with that of Faulkner-Skan profiles.

For small levels of actuation, the stability limits are in line with those other boundary layer profiles. However, as larger levels of plasma actuation are examined, it can be seen that they deviate from the behavior seen in other boundary layer profiles. This effect is likely due to the wall jet component of the velocity profile overpowering the boundary layer component, and transforming the flow in such a way that it cannot be compared to other boundary layers. Data is presented for the critical Reynolds number scaled by both $\delta^*_{Blasius}$ and the calculated value of δ^* for the velocity profile. The Reynolds number scaling does seem to make some difference in matching the current results to the universal correlation. However, once the velocity profile allows for significant wall jet like effects to develop, its stability diverges from that of more traditional boundary layers.

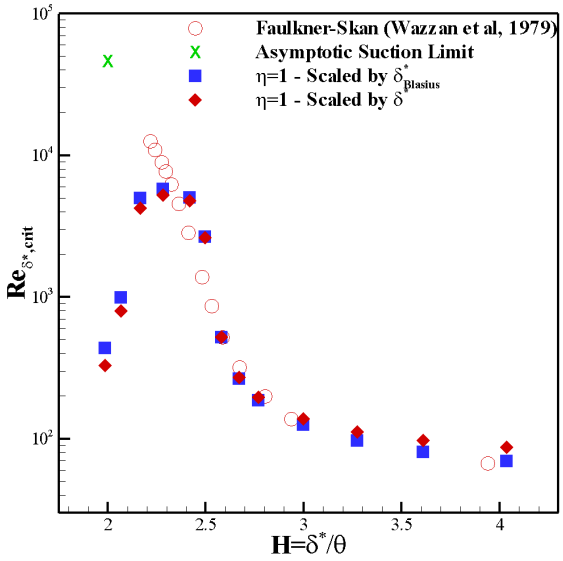

Figure 7. Comparison of current results to other boundary layer profiles.

E. Inviscid Instabilities

Up to this point, only viscous stability theory has been discussed. However, examining the velocity profiles presented in Fig. 1, it can be seen that there are instances where inflection points may occur in the profile. The presence of inflection points is typically indicative of an inviscid instability.[23] In order to better understand if the inflection points do pose a threat as far as allowing for inviscid instabilities, Fjørtoft's criterion is employed, where

$$\frac{\partial^2 u}{\partial x_2^2}(u_S - u) < 0 \tag{13}$$

indicates that an inviscid instability may exist for that boundary layer profile.

A wide range of combined wall jet/boundary layer profiles were created and analyzed by using Fjørtoft's criterion (Fig. 8) over 307,680 samples. It can be seen that an inviscid instability is nearly always predicted

for counter-flow actuation. Similarly, a majority of co-flow actuation also presents itself as being vulnerable to inviscid instabilities. Only when $\gamma = 0$, is the boundary layer certain to be viscidly stable. However, this is a trivial result, as $\gamma = 0$ corresponds to the Blasius boundary layer, which is known to be viscidly stable.

In spite of the possibility of creating an inviscid instability by pushing a wall jet in either direction, there is a significant region in γ and η where the flow is inviscidly stable (Fig. 8). As the wall jet is placed higher and higher in the boundary layer, the effects of the inflection points induced by the addition of the wall jet become less profound relative to the natural curvature of the boundary layer profile. Furthermore, the inflection point velocity, u_S is increased, and it is less likely that Fjørtoft's criterion will be met.

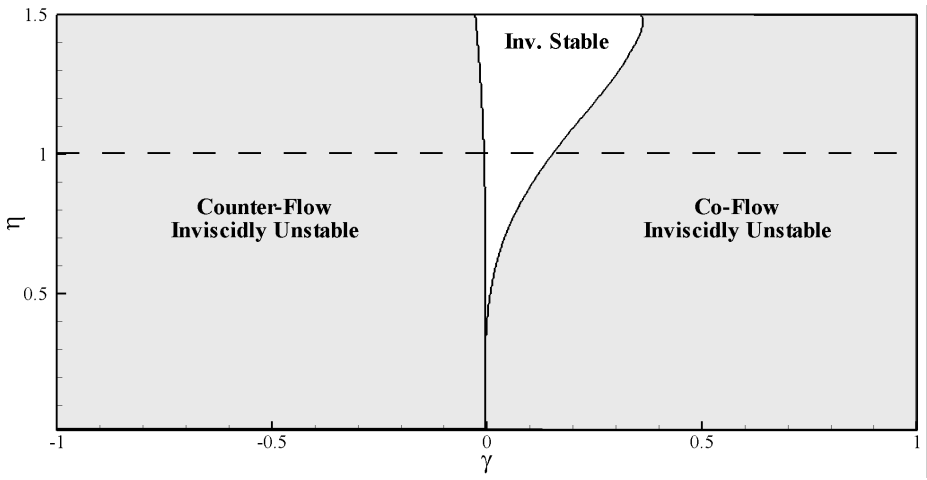

Figure 8. Fjørtoft's criterion applied to a wide range of wall jet/boundary layer velocity profiles.

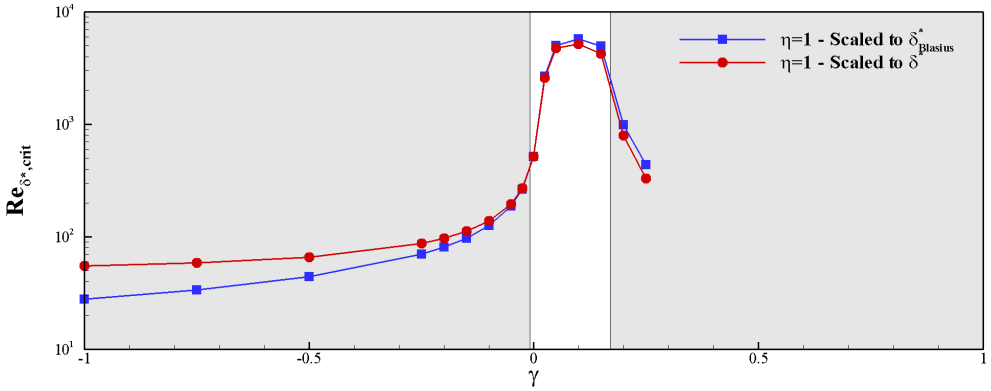

Figure 9. Critical Reynolds number for varying γ and $\eta = 1$. The shaded region is satisfied by Fjørtoft's criterion.

Comparing this map of the inviscid instability to the viscous analysis performed, it can be seen that the flow stability is augmented only when Fjørtoft's criterion is not satisfied (Fig. 9). When the inviscid instability is possible, viscous stability theory shows that the flow stability is diminished relative to that of the non-actuated boundary layer profile.

IV. Application to flow control

All of the analysis up to this point has been performed to determine how a plasma actuator can be used to modify the stability of a boundary layer. An understanding has been developed that low levels of actuation operated in the flow wise direction can be stabilizing. However, too much flow-wise actuation or even small amounts of counter-flow actuation can quickly destabilize the flow (Fig. 9). This indicates that there is a narrow range of control for flow stabilization, and moving outside of this range can easily lead to destabilization.

Numerical simulations have been performed using an Implicit Large Eddy Simulation (ILES) method[24] using the code FDL3DI. The flow over a flat plate was simulated with the addition of a plasma actuator. Two separate flow conditions were examined, with a single actuator placed in the flow. Under the two conditions, the actuator was placed at either a subcritical ($Re_x = 50,000$) or at an unstable ($Re_x = 100,000$) position along the length of the boundary layer. The actuation was oriented in a co-flow manner. A fine two dimensional mesh (801×151) was used which resolved the near wall boundary layer, the effects of a sharp leading edge, and the steady addition of momentum through a body force term. At the location of plasma actuation, there were 82 and 62 points in the boundary layer ($\delta_{99\%}$) for the lower and higher Reynolds number cases. The plasma actuation is modeled using a phenomenological model[25] of the body force in a method consistent with the description in.[24] The magnitude of the actuation was calibrated under quiescent conditions to acheive a particular value of γ immediately downstream of the actuator.

Results of these simulations were analyzed and values of γ and η were extracted for the two cases. It can be seen in Fig. 10a,d, that even though the initial value of γ may be high, it quickly decays at an exponential rate. This is good for flow stabilization. This initial decay of the velocity ratio moves the boundary layer profile away from the less stable regions of high γ and towards the more stable regions. However, as one moves downstream and the value of γ continues to decay to zero, the velocity profile eventually returns to the Blasius profile, and the gains in stability are lost. Examining the values of η, it can be seen that initially, a wall jet buried deep in the boundary layer will moves outwards. This is likely due to the stronger viscous effects near the wall removing the momentum in that region, as well as the slight wall normal velocity component of the boundary layer convecting the wall jet outwards. Again, this is a beneficial effect for flow stabilization. If one compares this to the location of potential inviscid instabilities shown in Fig. 8, the data shown here moves out of an inviscidly unstable region (high γ, low η) to a more inviscidly stable region (low γ, high η). Farther downstream, the boundary layer height ratio continues to move, but the wall jet is very weak and largely out of the boundary layer, so effects here are assumed to be negligible.

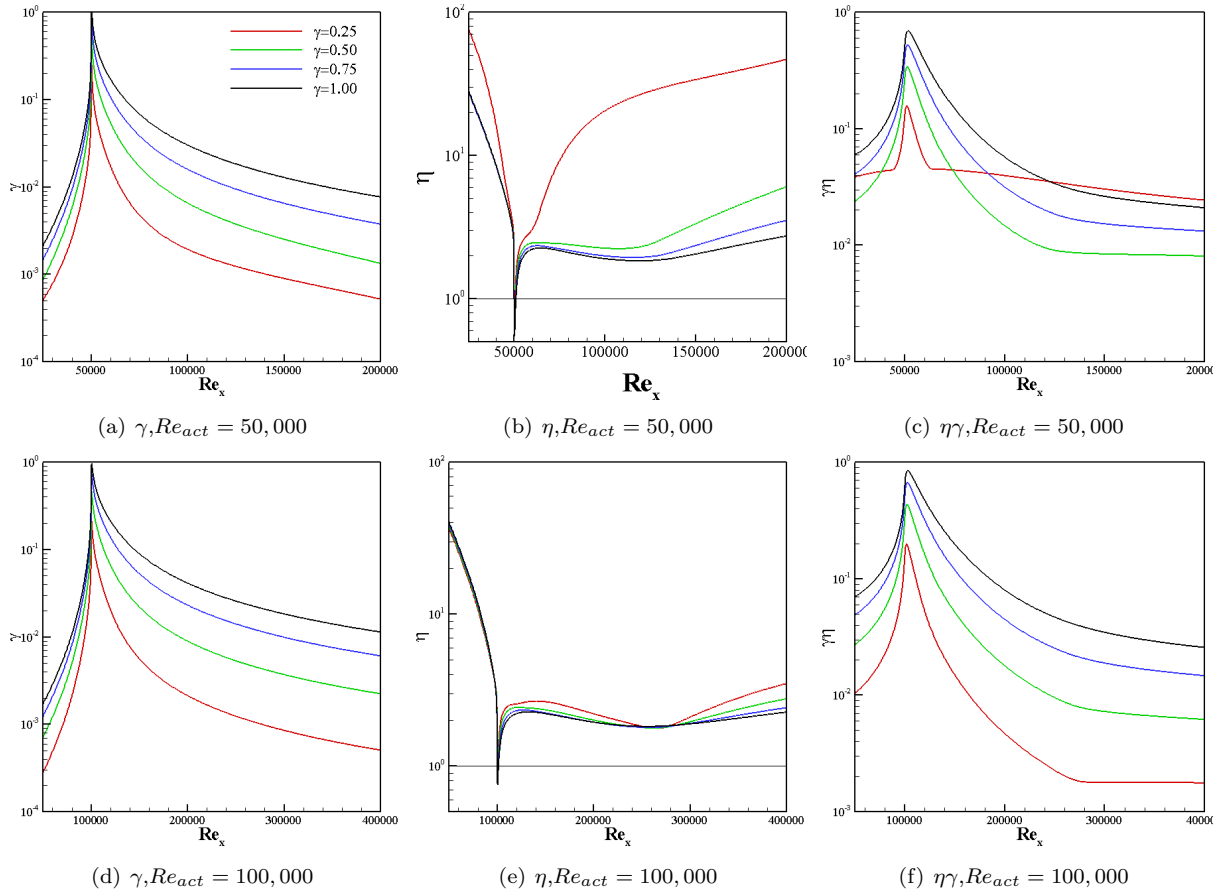

(a) γ,$Re_{act} = 50,000$ (b) η,$Re_{act} = 50,000$ (c) $\eta\gamma$,$Re_{act} = 50,000$

(d) γ,$Re_{act} = 100,000$ (e) η,$Re_{act} = 100,000$ (f) $\eta\gamma$,$Re_{act} = 100,000$

Figure 10. Extracted values of γ and η from simulated flows.

For counter flow operation of the plasma actuators, it can be assumed that the flow will quickly be destabilized, and transition augmented. However, this effect is not certain to happen. The flow reversal seen with counter flow actuation is only significant near the plasma actuator. Furthermore, these effects can also be assumed to quickly dissipate downstream of the actuator. So while the flow may be locally destabilized, global flow destabilization is not a definite effect.

This method of counter-flow actuation for flow destabilization has been used previously as a boundary layer trip.[26] However, in order to take advantage of plasma actuation as a trip for the flow, the Reynolds number of the boundary layer must be large enough to support unsteady and unstable effects, otherwise any instabilities that grow due to the operation of a counter flow oriented actuator will be lost.

V. Conclusions

The stability of a combined wall jet/boundary layer flow has been explored and analyzed using linear stability theory. Parameters classifying and a model of the velocity profile have been developed. The stability of the velocity profile has been formulated as an eigenvalue problem, and a parametric study performed calculating the neutral stability curves for various velocity profiles corresponding to higher and lower levels of plasma actuation.

In examining co-flow actuation, it was seen that the addition of plasma actuation stabilizes the flow up to a point. Beyond that point, the stability of the flow begins to decrease again, and the critical Reynolds number can be reduced to below that of the baseline boundary layer profile. While the destabilizing behavior is still in a viscous mode, the region of destabilizing behavior correlates well with the presence of an inviscid instability.

When counter flow actuation is performed, the addition of a wall jet is found to be highly destabilizing. Again, interactions with an inviscid instability are suggested to be of importance. It is also found that when the levels of actuation are high enough, the flow can be reversed. As the plasma actuation is further increased, absolute instabilities can develop, further showing the versatility of these devices for the manipulation of flow stability.

The effects of these devices have also been compared to the 'universal' correlation between the shape factor and boundary layer stability. It was found that strong agreement exists for relatively low levels of co-flow and up to strong levels of counter flow actuation. However, when the boundary layer begins to show distinct wall jet like effects, the stability diverges from that of the universal correlation.

The application of these devices for flow control applications has been discussed. The stabilization and destabilization effects hold significant potential and could be used to promote or delay boundary layer transition in a relatively simple manner.

Acknowledgments

The authors would like to acknowledge Dr. S. Balachandar for numerous helpful conversations while working on this study. The first author was supported by the University of Florida Graduate School Fellowship Award.

References

[1]Tollmien, W., "Über die Entstehund der Turbulenz," *Nachr. Ges. Wiss. Göttingen, Math.-Phys. Kl.*, 1929, pp. 21–44.

[2]Schlichting, H., "Zur Entstehung der Turbulenz bei der Plattenströmung," *Z. Angew. Math. Mech.*, Vol. 13, 1933, pp. 171–174.

[3]Schubauer, G. B. and Skramstad, H. K., "Laminar boundary-layer oscillations and transition on a flat plate," *Z. Angew. Math. Mech.*, Vol. 38, 1947, pp. 251–292.

[4]Gaster, M., "Nonparallel effects on boundary layer stability," *J. Fluid Mech.*, Vol. 66, 1974, pp. 465–480.

[5]Herbert, T. and Bertolotti, F. P., "Stability analysis of of nonparallel boundary layers," *Bulletin of the Amer. Phys. Soc.*, 1987.

[6]Roth, J. R., Sherman, D. M., and Wilkinson, S. P., "Boundary layer flow control with a one atmosphere uniform glow discharge surface plasma," *AIAA Paper 1998-328*, 1998.

[7]Corke, T. C., Enloe, C. L., and Wilkinson, S. P., "Dielectric Barrier Discharge Plasma Actuators for Flow Control," *Annual Review of Fluid Mech.*, Vol. 66, 2010, pp. 505–529.

[8]Moreau, E., "Airflow control by non-thermal plasma actuators," *J. of Phys. D: Appl. Phys.*, Vol. 40, 2007, pp. 605–636.

[9]Grundmann, S. and Tropea, C., "Active Cancellation of artificially induced Tollmien-Schlichting waves using plasma actuators," *Exp. in Fluids*, Vol. 44, 2008, pp. 795–806.

[10]Grundmann, S. and Tropea, C., "Experimental damping of boundary-layer oscillations using DBD plasma actuators,"

Intl. J. of Heat and Fluid Flow, Vol. 30, 2009, pp. 394–402.
[11]Gibson, B. A., Arjomandi, M., and Kelso, R. M., "The response of a flat plate boundary layer to an orthogonally arranged dielectric barrier discharge actuator," *J. Phys. D: Appl. Phys.*, Vol. 45, 2012.
[12]Albrecht, T., Grundmann, R., Mutschke, G., and Gunter, G., "On the stability of the boundary layer subject to a wall-parallel Lorentz force," *Phys. of Fluids*, Vol. 18, 2006.
[13]Duchmann, A., Reeh, A., Quadros, R., Kriegseis, J., and Tropea, C., "Linear Stability Analysis for Manipulated Boundary-Layer Flows using Plasma Actuators," 2010.
[14]Glauert, M. B., "The wall jet," *J. of Fluid Mech*, 1956.
[15]Schlichting, H. and Gersten, K., "Boundary Layer Theory, 8th Ed." 2000.
[16]Opaits, D., Zaidi, S., Shneider, M., Likhanskii, A., Edwards, M., and Macheret, S., "Surface plasma induced wall jets," *AIAA Paper 2010-0469*, 2010.
[17]Gaster, M., "A note of the relation between temporally-increasing and spatially-increasing disturbances in hydrodynamics stability," *J. Fluid Mech.*, Vol. 14, 1962, pp. 222–224.
[18]Patankar, S. V., "Numerical Heat Transfer and Fluid Flow," 1980.
[19]Orzag, S. A., "Accurate solution to the Orr-Sommerfeld stability equation," *J. of Fluid Mech.*, Vol. 50, 1971, pp. 689–703.
[20]Briggs, R. J., "Electron-Stream Interaction with Plasma," 1964.
[21]Bers, A., "Linear Waves and Instabilities," 1975.
[22]Wazzan, A. R., Gazley, C., and Smith, A. M. O., "Tollmien-Schlichting waves and Transition: heated and adiabatic wedge flows with applications to bodies of revolution," *Prog. in Aero. Sci.*, Vol. 18, 1979, pp. 351–392.
[23]Drazin, P. G. and Reid, W. H., "Hydrodynamic Stability," 1981.
[24]Rizzeta, D. P., Visbal, M. R., and Morgan, P. E., "A high-order compact finite-difference scheme for large-eddy simulations of active flow control," *Prog. in Aerospace Sci.*, Vol. 44, 2008, pp. 397–426.
[25]Shyy, W., Jayaraman, B., and Andersson, A., "Modeling of glow discharge-induced fluid dynamics," *J. Appl. Phys.*, Vol. 92, 2002, pp. 6434–6443.
[26]Rizzetta, D. P. and Visbal, M. R., "Large-Eddy Simulation of Plasma-Based Turbulent Boundary-Layer Separation Control," *AIAA J.*, Vol. 48, No. 12, pp. 2793–2810.